Human Molecular Genetics, 2012, Vol. 21, No. 13 **2923–2935**
doi:10.1093/hmg/dds118
Advance Access published on March 30, 2012

Clustered burst firing in *FMR1* premutation hippocampal neurons: amelioration with allopregnanolone

Zhengyu Cao[1], Susan Hulsizer[1], Flora Tassone[2,5], Hiu-tung Tang[2], Randi J. Hagerman[3,5], Michael A. Rogawski[4], Paul J. Hagerman[2,5] and Isaac N. Pessah[1,5,*]

[1]Department of Molecular Biosciences, School of Veterinary Medicine, [2]Department of Biochemistry and Molecular Medicine, School of Medicine, [3]Department of Pediatrics, School of Medicine, [4]Department of Neurology, School of Medicine and [5]Medical Investigations of Neurodevelopmental Disorders (MIND) Institute, University of California, Davis, CA 95616, USA

Received February 12, 2012; Revised and Accepted March 26, 2012

Premutation CGG repeat expansions (55–200 CGG repeats; preCGG) within the fragile X mental retardation 1 (*FMR1*) gene cause fragile X-associated tremor/ataxia syndrome (FXTAS). Defects in neuronal morphology and migration have been described in a preCGG mouse model. Mouse preCGG hippocampal neurons (170 CGG repeats) grown *in vitro* develop abnormal networks of clustered burst (CB) firing, as assessed by multielectrode array recordings and clustered patterns of spontaneous Ca^{2+} oscillations, neither typical of wild-type (WT) neurons. PreCGG neurons have reduced expression of vesicular GABA and glutamate (Glu) transporters (VGAT and VGLUT1, respectively), and preCGG hippocampal astrocytes display a rightward shift on Glu uptake kinetics, compared with WT. These alterations in preCGG astrocytes and neurons are associated with 4- to 8-fold elevated *Fmr1* mRNA and occur despite consistent expression of fragile X mental retardation protein levels at ~50% of WT levels. Abnormal patterns of activity observed in preCGG neurons are pharmacologically mimicked in WT neurons by addition of Glu or the mGluR1/5 agonist, dihydroxyphenylglycine, to the medium, or by inhibition of astrocytic Glu uptake with DL-*threo*-β-benzyloxyaspartic acid, but not by the ionotropic Glu receptor agonists, α-2-amino-3-(5-methyl-3-oxo-1,2-oxazol-4-yl) propanoic acid or *N*-methyl-D-aspartic acid. The mGluR1 (7-(hydroxyimino)cyclopropa [*b*]chromen-1a-carboxylate ethyl ester) or mGluR5 (2-methyl-6-(phenylethynyl)pyridine hydrochloride) antagonists reversed CB firing. Importantly, the acute addition of the neurosteroid allopregnanolone mitigated functional impairments observed in preCGG neurons in a reversible manner. These results demonstrate abnormal mGluR1/5 signaling in preCGG neurons, which is ameliorated by mGluR1/5 antagonists or augmentation of $GABA_A$ receptor signaling, and identify allopregnanolone as a candidate therapeutic lead.

INTRODUCTION

Fragile X syndrome (FXS) is the most common inherited form of cognitive impairment and a leading single-gene disorder associated with a high rate of autism (1,2). FXS is caused by trinucleotide (CGG) repeat expansions of >200 repeats (termed *full mutation*) within the 5′ non-coding region of the fragile X mental retardation 1 (*FMR1*) gene located on the X chromosome. Expansion CGG repeats >200 generally result in the hypermethylation of *FMR1* gene, which leads to transcriptional silencing and absence of fragile X mental retardation protein (FMRP) (3–5). Individuals with intermediate length CGG expansions, between 55 and 200 repeats (premutation), are typically unaffected by FXS but can display a range of clinical features including behavioral and cognitive abnormalities in children (6–9). Premutation carriers have a higher rate of primary ovarian insufficiency (fragile X-associated primary ovarian insufficiency—FXPOI) (10), and a substantial proportion experience a late-adult-onset

*To whom correspondence should be addressed at: Department of Molecular Biosciences, School of Veterinary Medicine, University of California, Davis, One Shields Avenue, Davis, CA 95616, USA. Tel: +1 5307526696; Fax: +1 5307524698; Email: inpessah@ucdavis.edu

neurodegenerative disorder, fragile X-associated tremor/ataxia syndrome (FXTAS) (11–13).

Premutation alleles of the *FMR1* gene are quite common in general population. Around 1:250–810 males and 1:130–250 females carry premutation alleles (14–16). In FXS families, ~46% of male premutation carriers and 16% of female carriers over 50 years of age will develop clinical features of FXTAS, with phenotypic penetrance increasing with age (16,17). Core clinical features of FXTAS include progressive gait ataxia and intention tremor with associated cognitive decline and executive dysfunction, peripheral neuropathy, dysautonomia and Parkinsonism (11,12,18,19). The absence of FXPOI and FXTAS symptoms in full mutation patents implies that FMRP deficiency *per se* is not responsible for premutation disorders and FXTAS. Instead, evidence from both human and animal studies suggests a direct toxic gain-of-function of premutation CGG (preCGG) alleles due to an increase in the CGG-repeat-containing *FMR1* mRNA (20–22). Consistent with this hypothesis, characteristic intranuclear inclusions found in neuronal and glia cells of FXTAS cases (23,24) have been demonstrated to contain *FMR1* mRNA (25). Additionally, the expanded CGG repeat-RNA is sufficient to form the intranuclear inclusions in both primary neural progenitor cells and established neural cell lines (26), and expression of expanded CGG repeats in Purkinje neurons produces intranuclear inclusions, neurodegeneration and motor deficits (27).

Knock-in (KI) mouse models have been developed. In one mouse model, a native 9–10 CGG repeat allele in the homologous *Fmr1* gene was replaced with CGG expansion repeats that can vary from 100 to >300 in size from generation to generation (28). Another KI mouse model was developed wherein CGG-CCG repeats were serially ligated in exon 1 of the endogenous mouse *Fmr1* gene (29). Similar to human premutation carriers, the hippocampus of premutation mice exhibits elevated *Fmr1* mRNA and normal to 50% reductions in FMRP compared with wild-type (WT), even in mice with large (150–190) repeats (20,21,29). The premutation mouse models do not fully recapitulate human FXTAS (28); however, they do show progressive deficits in processing spatial and temporal information, cognitive deficits (30), motor deficits (31) and hyperactivity (32). *Ex vivo* studies also showed ubiquitin-positive intranuclear inclusions in neurons and astrocytes are neuropathologic hallmarks of FXTAS in both human (23,24,25,33) and mouse brains (20,29,34). These ubiquitin-positive intranuclear inclusions were found in both neurons and astrocytes in preCGG mice *in vivo*. PreCGG mice exhibit altered embryonic neocortical development with migration defects in the neocortex and altered expression of neuronal lineage markers (35). Hippocampal neurons cultured from preCGG mice show impairments in dendritic complexity and an altered architecture of synapsin puncta prior to neurodegeneration (36); however, the functional consequences of early-onset morphologic alterations in preCGG neurons have not been investigated. PreCGG mice display upregulated mRNA levels of many components of GABAergic system in the cerebellum but not in the cortex (37), suggesting an altered inhibitory neuronal transmission in the preCGG mice model.

Here, we report that hippocampal neurons cultured from hemizygous male preCGG mice (170 CGG repeats) have deficiencies in neuronal vesicular GABA and glutamate (Glu) transporters (VGAT and VGLUT1) and develop abnormal burst firing electrical activity consisting of clustered patterns of spontaneous synchronized Ca^{2+} oscillations, not typical of neurons cultured from male WT mice. Exposure of WT neuronal cultures to pharmacologic agents that inhibit Glu uptake, activate mGlu R1/5, or inhibit $GABA_A$ receptors, all result in electrical firing behavior that phenocopies clustered burst (CB) firing behavior observed in preCGG neurons. These data provide functional evidence of an imbalanced excitatory–inhibitory neurotransmission in preCGG neurons. The mGluR1 (7-(hydroxyimino)cyclopropa[*b*]chromen-1a-carboxylate ethyl ester—CPCCOEt) or mGluR5 (MEPP) antagonists reversed CB firing. Furthermore, treatment of preCGG neurons with the neurosteroid allopregnanolone, a positive allosteric modulator of $GABA_A$ receptors, mitigates the functional electrical impairments observed in preCGG neurons in a reversible manner, identifying a possible therapeutic strategy for ameliorating abnormal neuronal activity in individuals with the premutation.

RESULTS

PreCGG neurons express elevated *Fmr1* mRNA and intermediate levels of FMRP

Western blotting with a chicken monoclonal antibody detects FMRP (38) in the lysate of astrocyte cultures and astrocyte-neuronal co-cultures with the major band at 72 kDa (Fig. 1A), a band absent in the brain lysate of FMRP knockout mice, a model of FXS (data not shown). When normalized to the intensity of β-actin, hippocampal neurons cultured from preCGG mice with ~170 CGG expansion express 46.5 ± 3.2 and 51.4 ± 0.1% of the FMRP levels found in respective WT neurons measured at 14 days *in vitro* (DIV) and 21 DIV. Compared with WT, preCGG astrocytes express 55.8 ± 6.6% of the level of FMRP (Fig. 1B). Results from RT–PCR analyses show that premutation cultures (mean expansion 175 CGG repeats) show 4.1-, 7.6- and 8.4-fold higher *Fmr1* mRNA levels than the corresponding WT astrocyte and 14 as well as 21 DIV hippocampal neuronal cultures, respectively (Fig. 1C).

Premutation hippocampal neurons display prominent CB firing behavior

Simultaneous extracellular recordings of electrical activity from multiple sites within the neuronal cultures with a high spatial resolution provide a robust measure of network activity and connectivity (39). Electrical firing activity in cultures isolated from WT and preCGG hippocampus is measured using 64-electrode multielectrode arrays (MEAs) by converting electrical field potential recordings to raster plots as described in Materials and Methods and Supplementary Material, Figure S1. By culture day 7 DIV, both WT and preCGG hippocampal neurons display similar patterns of spontaneous electric activity comprising infrequent synchronized bursts of field potentials, mixed with desynchronized random spiking (Fig. 2A and B). Neither spike frequency nor burst duration differs between WT and preCGG cultures at 7 DIV

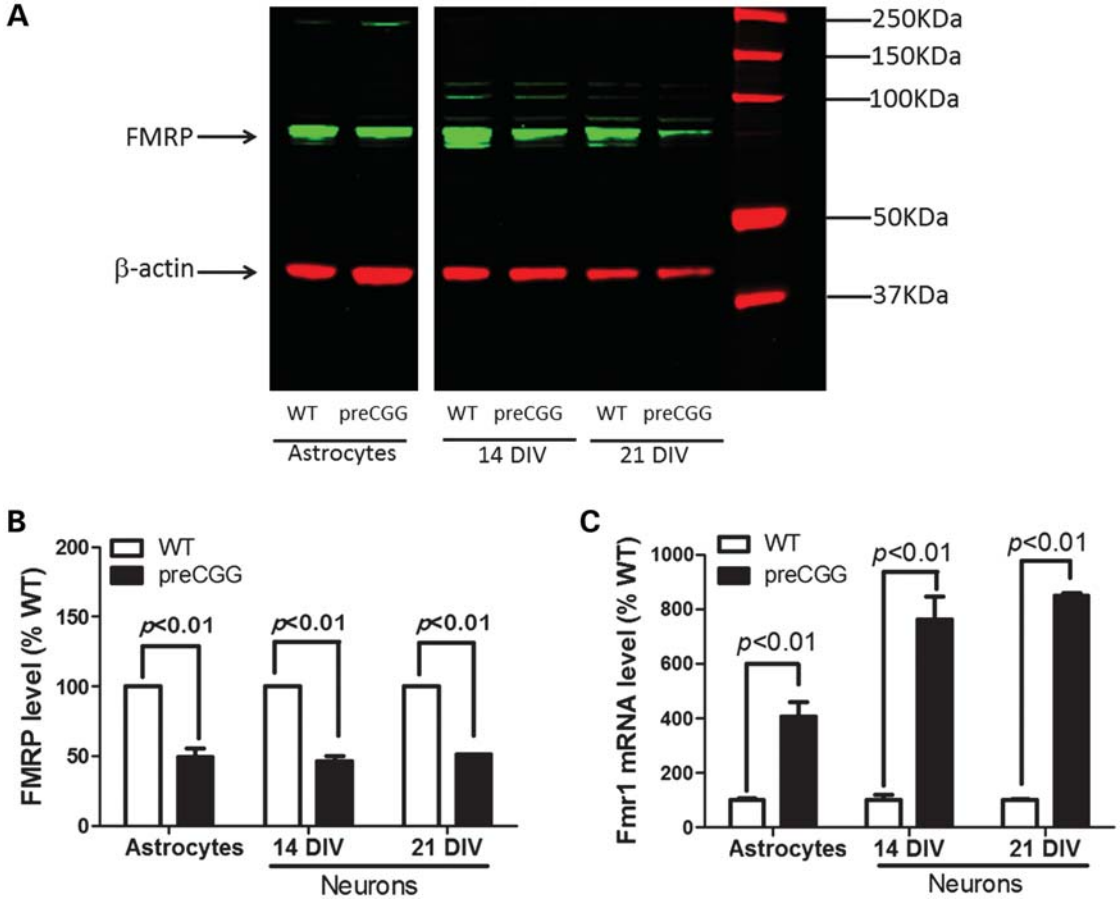

Figure 1. Premutation cultures express higher levels of *Fmr1* mRNAs with decreased FMRP proteins compared with WT paired cultures. (**A**) Representative western blot in paired cultures of WT and preCGG hippocampal astrocytes as well as neurons. The band with molecular weight around 72 kDa is FMRP. (**B**) Quantification of FMRP expression levels relative to β-actin in paired WT and preCGG cultures of hippocampal astrocytes, and 14 and 21 DIV neuronal cultures. Data were pooled from two independent cultures. (**C**) Fmr 1 mRNA comparison between WT and preCGG paired cultures of hippocampal astrocytes and 14 as well as 21 DIV neurons. Data were pooled from two independent cultures, each performed in duplicate.

(Fig. 2C and D). Synchronized firing activity increases in frequency and duration as neuronal networks matured by 21 DIV. At 21 DIV, preCGG hippocampal neurons display a distinct firing pattern composed of intense CBs interspersed with brief periods of quiescence (Fig. 2A and B). The percentage of MEAs reporting the CB firing pattern is significantly higher in the preCGG neuronal cultures than in WT neurons. With WT hippocampal neurons, $<10\%$ of the MEAs recorded ($n = 37$) show CB firing patterns lasting 10 s or longer, compared with $>60\%$ ($n = 26$) of the MEAs, with preCGG neurons displaying CB firing lasting 10 s or longer (Supplementary Material, Fig. S2, black bars). PreCGG neurons (21 DIV) display neuronal network activity having a higher spike frequency (WT $= 1.55 \pm 0.22$ spikes s^{-1}, $n = 26$ versus preCGG $= 4.35 \pm 0.64$ spikes s^{-1}, $n = 37$, $P < 0.01$) and a longer mean burst duration (WT $= 0.43 \pm 0.10$ s, $n = 26$ versus preCGG $= 1.67 \pm 0.24$ s, $n = 37$, $P < 0.01$).

Altered patterns of spontaneous Ca^{2+} oscillation in preCGG hippocampal neurons

Cultured hippocampal neurons display spontaneous synchronous Ca^{2+} oscillations (40). We simultaneously evaluated the spontaneous Ca^{2+} dynamics in WT and preCGG neurons cultured on 96-well plates, using the FLIPR TETRA® high-throughput cellular imaging system. Similar to the CB firing behavior observed in MEA measurements, preCGG hippocampal neurons (14 DIV) display temporally clustered Ca^{2+} oscillations interspersed with quiescent periods in nearly 90% of the wells measured ($n = 93$), a pattern seen in only 23.9% of the wells ($n = 71$) containing WT hippocampal neurons (Fig. 3).

PreCGG hippocampal neurons express less VGLUT1 and VGAT

VGLUT and VGAT are transporters that are expressed primarily in excitatory and inhibitory neurons (41,42) and are responsible for the uptake of Glu and GABA into presynaptic vesicles (43,44). Disruption in the balance between an excitatory and inhibitory transmission has been shown to influence overall neuronal activity, leading to abnormal burst firing in neurons (45). We measured the expression levels of VGLUT1 and VGAT, using western blot analysis. Figure 4A and B shows that at 7 DIV, both VGLUT1 and VGAT expression are slightly higher in preCGG compared with WT

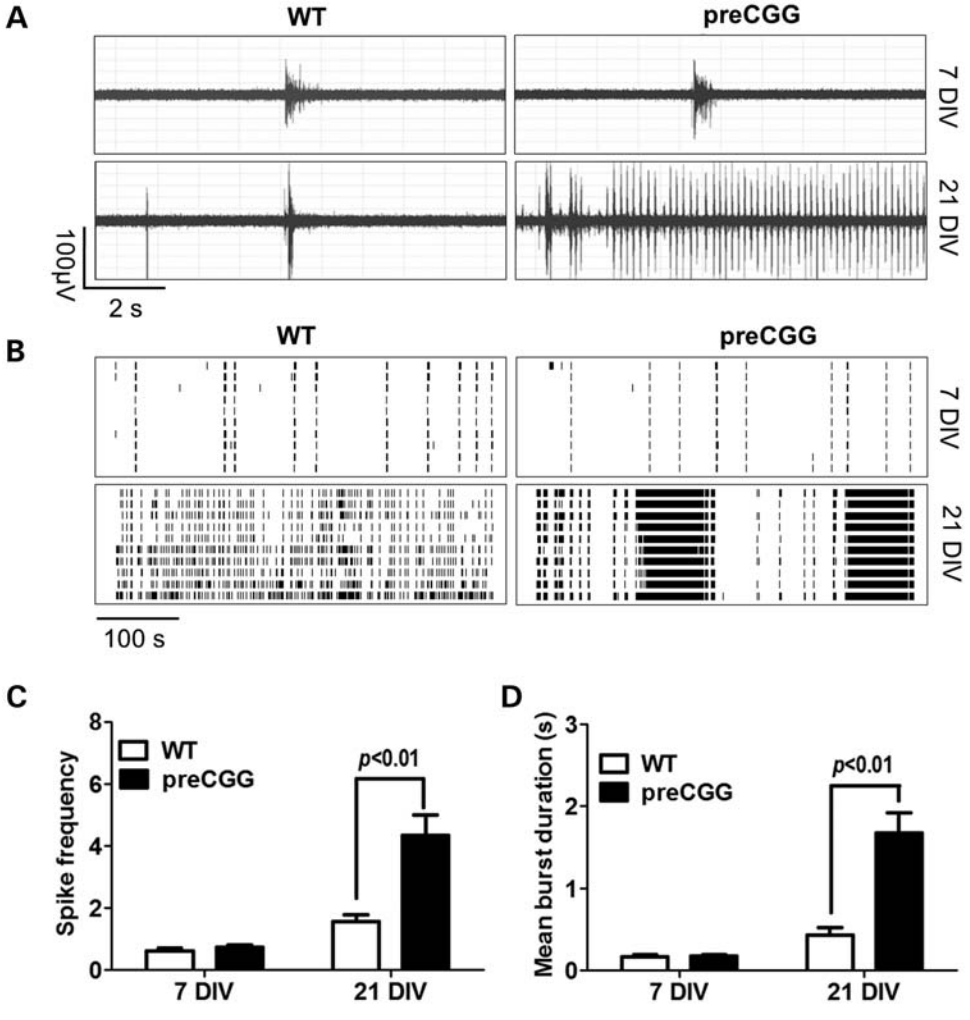

Figure 2. Hippocampal neurons with CGG expansion predominantly display a pattern of spontaneous field potential activity having CB firing. (**A**) Representative traces of firing for WT and preCGG hippocampal neurons at 7 and 21 DIV in a 10 s epoch. (**B**) Representative raster plots for the neuronal firing of WT and preCGG hippocampal neurons at 7 and 21 DIV. (**C** and **D**) Quantification of the spike frequency and mean burst duration for WT and preCGG hippocampal neurons at 7 and 21 DIV. Summary data were from 26 MEAs for WT and 37 MEAs for preCGG hippocampal neurons.

neurons. However, by 21 DIV, preCGG neurons display significantly lower expression of both VGLUT1 and VGAT than WT, whereas the ratios of VGAT to VGLUT1 do not differ between genotypes. However, the VGAT/VGLUT1 ratio declined in both genotypes from 7 to 21 DIV (Fig. 4C). The trajectories of *in vitro* expression for VGAT and VGLUT1 diverge. VGAT decreases 27.0% in preCGG but only 6.0% in WT between 7 and 21 DIV (Fig. 4D). In contrast, VGLUT1 increases 280.1 and 203.3% in WT and preCGG neurons, respectively, during this DIV period (Fig. 4D).

PreCGG hippocampal astrocytes display lower affinity of Glu uptake

Astrocyte transporters remove Glu from the synapse (46). We compared Glu uptake kinetics of hippocampal astrocytes cultured from WT and preCGG male pups. Figure 5A shows similar Glu uptake in WT (126.1 ± 1.7 nmol/mg protein) and preCGG astrocytes (126.9 ± 2.2 nmol/mg protein) for 30 min. Preincubation (25 min) of astrocytes with DL-*threo*-β-benzyloxyaspartic acid (TBOA) and L-*trans*-pyrrolidine-2,4-dicarboxylic acid (L-*trans*-PDC), non-selective inhibitors of Glu uptake, inhibited Glu uptake 50 and >90%, respectively, regardless of genotype. Initial experiments indicate that 100 μM Glu is sufficient for linear rates of uptake for at least 10 min (data not shown). Therefore, for kinetics analysis, the incubation time was shortened to 10 min. Figure 5B shows that the V_{max} for Glu does not differ between WT and preCGG hippocampal astrocytes, although preCGG astrocytes display a significant lower affinity for Glu (preCGG $K_m = 28.4 \pm 2.2$ μM, mean ± SEM; WT $K_m = 20.0 \pm 2.8$ μM, mean ± SEM, $n = 4$, $P < 0.01$).

Modulation of Glu and GABA signaling produces CB firing pattern in WT neurons

Since preCGG astrocytes may have impaired Glu clearance, we investigated the influence of Glu on the neuronal firing activity in WT neurons. The acute application of 100 μM of Glu

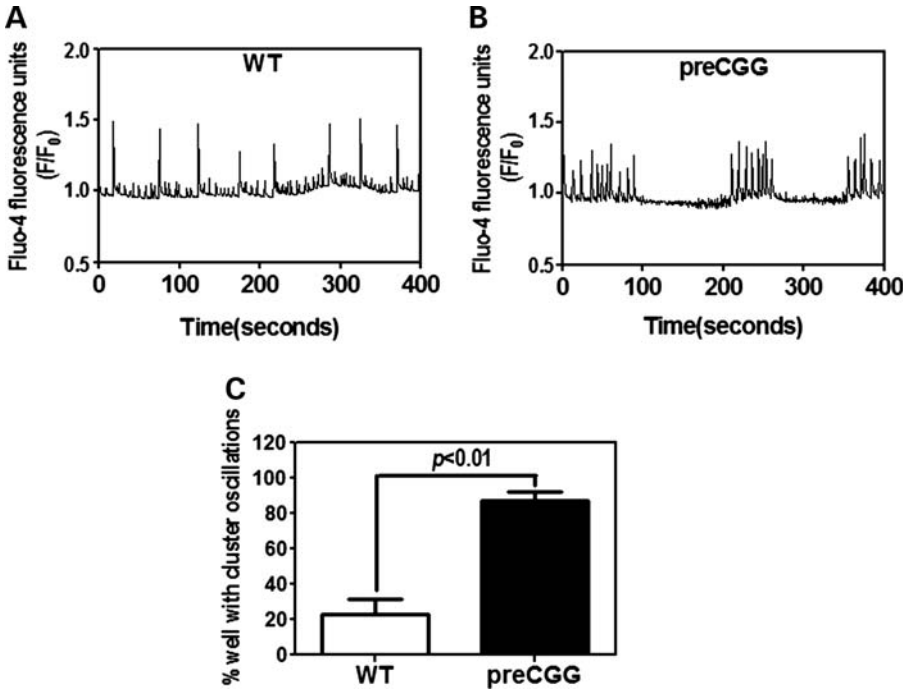

Figure 3. Hippocampal neurons with CGG expansion predominately display clustered Ca^{2+} oscillations. Representative intracellular Ca^{2+} oscillations in WT (**A**) and preCGG (**B**) hippocampal neurons measured at 14 DIV. (**C**) Quantification of the percentage of wells displaying clustered Ca^{2+} oscillations. These data were summarized from five independent cultures with a total number of wells of 71 and 93 for the WT and preCGG hippocampal neurons, respectively.

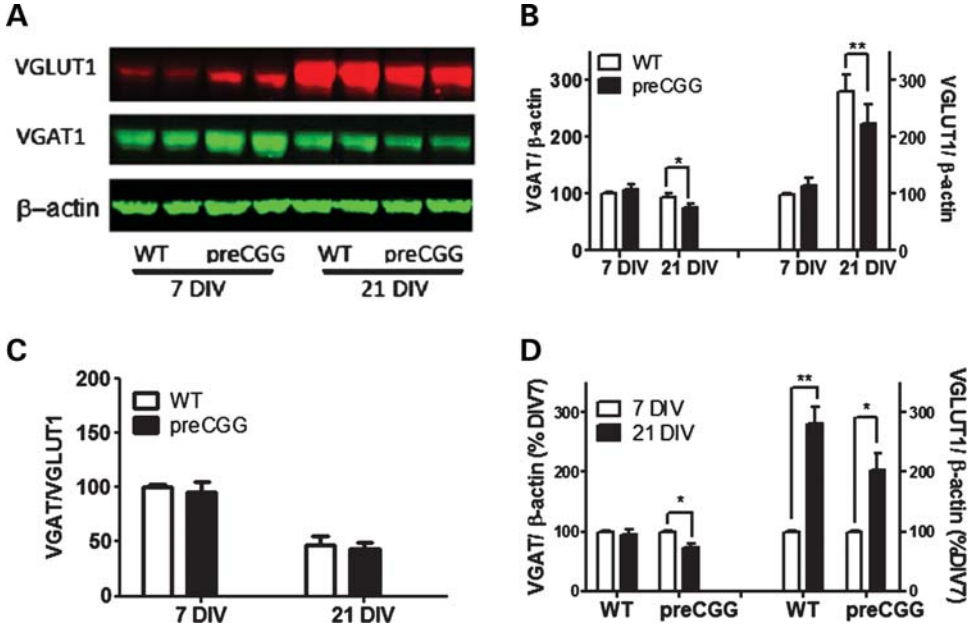

Figure 4. 21 DIV hippocampal neurons with CGG expansion display decreased expression levels of VGAT and VGLUT1. (**A**) Representative western blots for VGAT and VGLUT1. (**B**) Quantification of the expression levels for VGAT and VGLUT1. These data were normalized to the expression levels of VGAT or VGLUT1 on 7 DIV WT neurons. (**C**) Quantification of the ratio of VGAT over the VGLUT1 expression level. (**D**) Quantification of the developmental change of VGAT and VGLUT1. These data were normalized to the expression levels of respective 7 DIV neurons for each genotype. $n = 4$ from three separate culture days.

to the WT neurons produced a CB firing pattern. Glu significantly increased the spike rates from 1.44 ± 0.24 to 6.77 ± 1.24 spikes s^{-1} as well as the mean burst duration from 0.23 ± 0.01 to 4.52 ± 0.76 s (Fig. 6C). To test whether the rightward shift of Glu uptake observed in preCGG astrocyte cultures affects neuronal firing, we mimicked the Glu transport

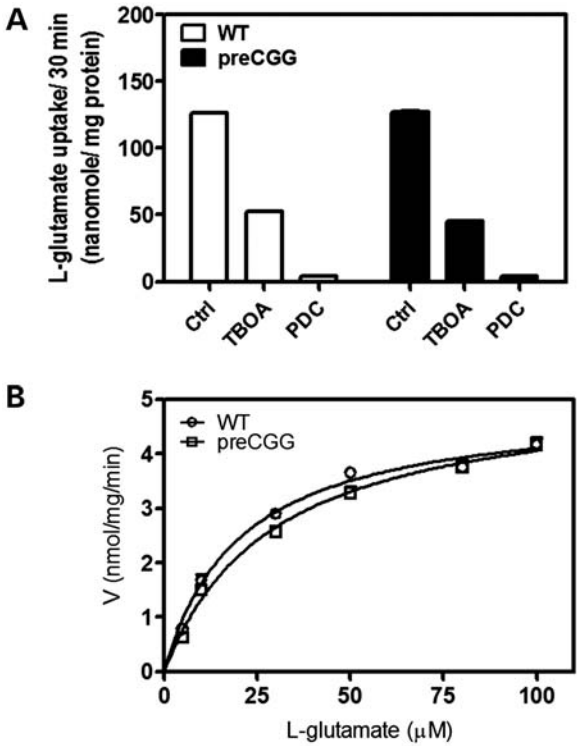

Figure 5. Glu uptake in pure hippocampal astrocyte cultures. (**A**) Non-selective Glu transporter inhibitors, DL-TBOA (1 mM) and L-*trans*-PDC (1 mM), blocked Glu uptake in both WT and preCGG hippocampal astrocytes. These data were repeated in two cultures, in triplicate, with similar results. (**B**) Kinetic analysis for Glu uptake in WT and preCGG hippocampal astrocytes. The experiments were repeated in four independent cultures performed in triplicate with similar results. Uptake as a function of Glu concentration was fitted by the Michaelis–Menten equation. The V_{max} values for Glu uptake do not show a statistically significant difference between WT and preCGG hippocampal astrocytes. However, the K_m value was shifted from 20.0 ± 2.8 μM for WT to 28.4 ± 2.2 μM for preCGG ($n = 4$, $P < 0.01$).

impairment in WT neurons by introducing TBOA, a non-selective, competitive Glu uptake antagonist. Figure 6D and E shows that the application of TBOA (100 μM) produced a CB firing pattern in WT hippocampal neurons, increasing the spike rate from 1.05 ± 0.10 to 2.42 ± 0.29 spikes s^{-1}, as well as the mean burst duration from 0.42 ± 0.03 to 0.84 ± 0.07 s. Considered together, these data demonstrate that pharmacologically mimicking the dysfunction of Glu signaling could reproduce the CB firing pattern observed in the premutation neurons.

We next examined the roles of ionotropic [*N*-methyl-D-aspartic acid (NMDA) and α-2-amino-3-(5-methyl-3-oxo-1,2-oxazol-4-yl) propanoic acid (AMPA)] Glu receptors and type-I metabotropic Glu receptors (mGluRs) in producing a CB firing pattern by application of specific agonists. As shown in Supplementary Material, Figure S3A, the application of NMDA produced a robust increase on the spike rate; however, rather than forming a CB firing pattern, these spikes were evenly distributed over the recording period. The application of a low concentration of AMPA (100 nM) produced a slight increase of the spike rate. These spikes were mostly asynchronous and randomly spaced and did not form a CB pattern. A higher concentration of AMPA (1 μM) eliminated most electric activity (Supplementary Material, Fig. S3B). The actions of NMDA and AMPA observed here are similar to those observed previously in cortical neurons (47).

Figure 7 shows that the application of type-I mGluR activator, dihydroxyphenylglycine (DHPG) (10 μM), produced a CB firing pattern in WT hippocampal neurons, increasing the spike frequency from 0.85 ± 0.08 to 21.79 ± 1.09 spikes s^{-1} as well as the mean burst duration from 0.31 ± 0.02 to 1.05 ± 0.02 s. These data demonstrate that the type-I mGluRs play a key role in the generation of the CB firing pattern.

Reduced expression levels of VGAT could decrease GABA levels in presynaptic stores and lead to reduced strength and efficacy of GABA release. To assess the role of $GABA_A$ receptors, we pharmacologically suppressed the $GABA_A$ receptor function to mimic the reduced GABA signaling observed in premutation hippocampal neurons, using picrotoxin, a specific noncompetitive antagonist of $GABA_A$ receptors. Figure 8 shows that the application of picrotoxin (100 μM) did produce a CB firing pattern in WT hippocampal neurons, although the duration of the cluster is shorter than those observed in preCGG hippocampal neurons. Picrotoxin alone increased the spike rate from 0.61 ± 0.06 to 1.83 ± 0.02 spikes s^{-1} and the mean burst duration from 0.30 ± 0.02 to 0.64 ± 0.01 s, respectively. The application of picrotoxin (100 μM) and DHPG (10 μM) together in WT hippocampal neurons produced a robust CB firing pattern similar to the one observed in premutation hippocampal neurons with an increased spike rate (from 0.61 ± 0.06 to 7.7 ± 0.57 spikes s^{-1}) as well as a longer mean burst duration (from 0.30 ± 0.02 to 1.27 ± 0.06 s). These data together demonstrate that the manipulation of either Glu or GABA signaling in WT cultures recapitulates CB firing patterns in preGCC neurons, thereby implicating an altered excitatory–inhibitory balance in preCGG hippocampal neuronal transmission.

Suppression of type-I mGluRs function or enhancement of $GABA_A$ receptors activity rescues the CB phenotype in preCGG hippocampal neurons

Given the pivotal roles of type-I mGluRs and $GABA_A$ receptors signaling in the generation of the CB firing pattern, we next evaluated the neuronal firing activity after the suppression of type-I mGluR activity or the enhancement of $GABA_A$ receptor activity in preCGG hippocampal neurons. Figure 9A and B shows that the application of 2-methyl-6-(phenylethynyl)pyridine hydrochloride (MPEP), an antagonist of mGluR5 receptors, inhibited the spike rate and the mean burst duration in a concentration-dependent manner, reversing CB firing patterns to a randomly distributed burst firing pattern seen in WT cultures. Similarly, CPCCOEt, an mGluR1 antagonist, also suppressed the spike firing rate as well as the mean burst duration, thereby mitigating the CB firing pattern to a randomly distributed burst firing pattern observed in WT neurons.

We next evaluated the influence of allopregnanolone, a positive allosteric modulator of the postsynaptic $GABA_A$ receptors (48), on the electric firing pattern of preCGG hippocampal neurons. Figure 10A and B shows that

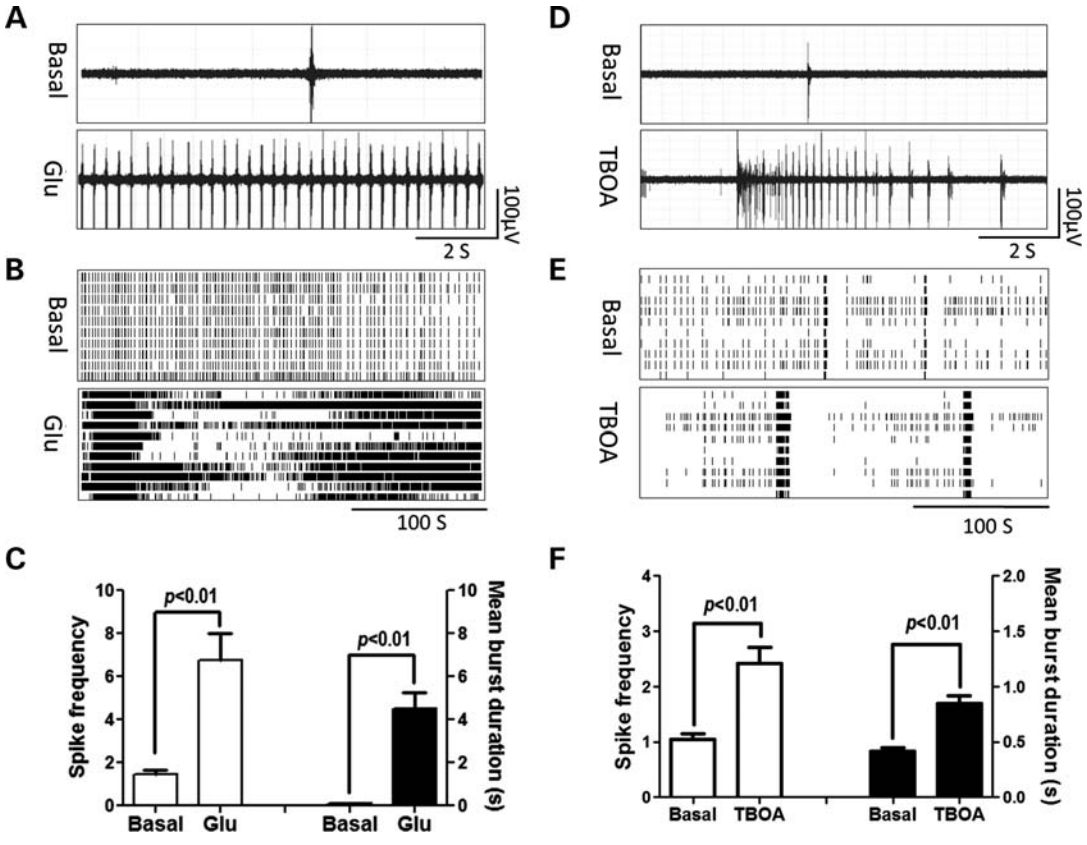

Figure 6. Glu and TBOA induce CB firing pattern in WT hippocampal neurons. (**A** and **D**) Representative trace for firing activity before and after WT hippocampal neurons exposed to Glu (100 μM) or TBOA (100 μM), respectively. (**B** and **E**) Representative raster plots for the neuronal firing before and after WT hippocampal neurons exposed to Glu or TBOA, respectively. (**C** and **F**) Quantification of the spike frequency (left *Y* axis) and mean burst duration (right *Y* axis) for WT hippocampal neurons before and after Glu or TBOA exposure, respectively. Data were repeated twice in duplicate with similar results.

allopregnanolone suppressed the CB firing pattern of preCGG hippocampal neurons (reducing the spike rate as well as the mean burst duration) in a concentration-dependent and reversible manner.

DISCUSSION

In this study, we have demonstrated that hippocampal neurons cultured from preCGG mice display a high penetrance for CB electrical spiking activity and abnormal patterns of spontaneous Ca^{2+} oscillations under basal culture conditions. Functional differences in preCGG neurons are observed in the presence of significantly elevated *Fmr1* mRNA and moderate levels of FMRP expression that are consistent with the previous findings in brain lysates and neuronal cultures prepared from KI mice expressing CGG repeats in the premutation range (4,21,36,49), and also consistent with findings from human premutation carriers and FXTAS patients (22,25). Therefore, the presence of both significantly elevated *Fmr1* mRNA and intermediate levels of FMRP models the human condition (22,25) and distinguishes preCGG hippocampal neurons and astrocytes from the FXS mouse model. Although prior studies have emphasized a toxic gain-of-function effect of elevated messenger RNA associated with the premutation, the current results from mouse preCGG hippocampal neurons also support a role of reduced FMRP in alterations of brain activity recently reported by Hessl *et al*. (50) using functional MRI of amygdala of premutation carriers.

The principal mechanisms contributing to the defects in basal electrical activity exhibited by preCGG neurons appear to be associated with a gain-of-function in type-I mGluRs and/or a loss-of-function in $GABA_A$ receptor signaling. This conclusion is supported by data indicating that (i) type-I mGluR receptor agonist DHPG, but neither NMDA nor AMPA receptor agonists, increased CB firing patterns in WT neurons with an increased spike rate and a mean burst duration similar to those observed in preCGG hippocampal neurons; (ii) selective mGluR1/5 antagonists (CPCCOEt and MPEP) abrogated CB activity in preCGG neurons; (iii) preCGG astrocytes have impaired Glu uptake; (iv) WT cultures exposed to the astrocyte Glu transport competitive antagonist TBOA produced CB firing patterns indistinguishable from those of preCGG neurons; (v) $GABA_A$ receptor block with picrotoxin phenocopied the CB firing behavior observed in preCGG neurons; and (vi) the allosteric $GABA_A$ receptor enhancer allopregnanolone essentially restored WT electrical spiking patterns.

These functional deficits are directly pertinent to the altered patterns of neuronal complexity reported earlier using the same *in vitro* preCGG model (36), and possibly contribute to migration defects in the neocortex of embryonic preCGG

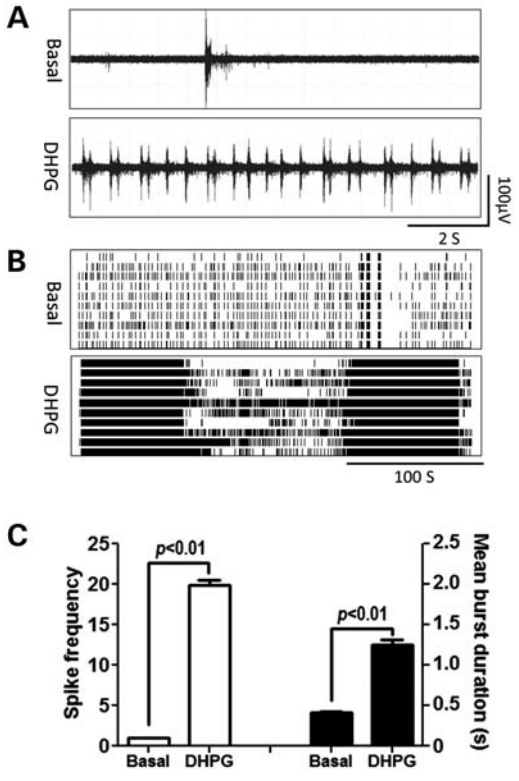

Figure 7. DHPG produces CB firing pattern in WT hippocampal neurons. (**A**) Representative trace for firing activity before and after WT hippocampal neurons exposed to 10 μM DHPG. (**B**) Representative raster plots for the neuronal firing before and after DHPG exposure. (**C**) Quantification of the spike frequency (left *Y* axis) and mean burst duration (right *Y* axis) for WT hippocampal neurons before and after DHPG exposure. Data were repeated twice in duplicate with similar results.

mice (35). Abnormal electrical firing patterns of neural networks could perhaps promote the seizures and developmental problems, including autism spectrum disorders and attention deficit hyperactivity disorder, seen in a subgroup of young premutation boys (8,51). Neuronal activity is essential for the normal neuronal migration (52), dendritic growth (53) and synaptic plasticity (54), processes mediated by spatially and temporally orchestrated intracellular Ca^{2+} signals. Cultured hippocampal neurons display spontaneous, synchronous Ca^{2+} oscillations (40) that are spaced at regular temporal intervals (this study). However, preCGG neurons exhibit synchronized clusters of Ca^{2+} oscillations that appear to coincide with intense CB firing. Low-to-moderate intracellular Ca^{2+} signals promote dendritic growth, whereas more intense Ca^{2+} signals have been proposed to cause dendritic retraction (55,56). Therefore, the abnormal CB electrical activity and abnormal patterns of spontaneous Ca^{2+} oscillations observed in preCGG hippocampal neurons are likely to contribute, at least in part, to impaired dendritic growth and synaptic architecture, including increased puncta volumes in presynaptic synapsin and postsynaptic phalloidin (36).

A balance between an excitatory and inhibitory synaptic transmission tightly controls spontaneous neuronal activity in hippocampal neurons. In simulations of neural networks, the manipulation of excitatory and inhibitory inputs produced distinct neuronal burst firing behaviors, including CBs (45), similar to those exhibited by preCGG neurons. CB firing activity is pronounced in preCGG neurons by 21 DIV at which time VGAT and VGLUT, markers of excitatory and inhibitory neurons, are expressed at significantly lower levels than in WT neurons. The ratio of VGAT/VGLUT does not differ between preCGG and WT at either 7 or 21 DIV, suggesting that a shift in the relative composition of glutamatergic and GABAergic neurons in the preCGG cultures is not responsible for CB firing activity. PreCGG neurons express 20.2% lower VGLUT1 relative to that on WT at 21 DIV, but such a modest reduction of VGLUT1 protein, the dominant isoform expressed in adult hippocampal neurons (57,58), is unlikely to have an influence on the basal Glu transmission (59), especially when considering the pronounced developmental upregulation of VGLUT1 expression observed between 7 and 21 DIV with both WT and preCGG neuronal cultures. The developmental upregulation of VGLUT1 observed in our *in vitro* study is consistent with the previous findings in the rat cerebral cortex and human dorsolateral prefrontal cortex (60,61).

VGAT expression remains unchanged as WT hippocampal neurons mature *in vitro*, an observation consistent with developmental studies in the human brain (61). In contrast, VGAT levels decrease nearly 27% from 7 to 21 DIV in preCGG neurons. Reduced expression of VGAT could result in insufficient re-uptake of GABA to presynaptic vesicles, negatively influencing the strength of the GABAergic synaptic transmission (43). Although impaired GABAergic synaptic function in preCGG neurons in combination with impaired Glu buffering by preCGG astrocytes could contribute to their CB firing pattern and clustered Ca^{2+} oscillations, we cannot discount the contributions of defects in mGluR1/5 and/or $GABA_A$ signaling pathways to preCGG impairments, especially given our results with pharmacologic modulation of their receptors. Ca^{2+} signaling dysregulation in FMRP-null models of FXS have been recently described (62,63). Defects in activity-dependent Ca^{2+} influx and Ca^{2+} store release have been demonstrated in the null *Drosophila FMR1* brain mushroom body and are dependent on the developmental stage (62). High-frequency stimulation of hippocampal CA3 neurons in the *Fmr1* knock-out mouse model significantly enhanced Ca^{2+} influx after the first few stimuli (63). These effects have been ascribed to the loss of FMRP expression. However, in our preCGG mouse model, there is substantial FMRP expression (~50% of WT levels) in both preCGG hippocampal astrocytes and neurons. Although we cannot rule out that intermediate levels of FMRP in preCGG neurons could contribute to CB activity and altered Ca^{2+} oscillatory behavior, this phenotype is more likely a consequence of a gain-of-function imparted by the ~8-fold increase in expanded CGG-repeat *Fmr1* mRNA or a combination of both intermediate FMRP levels and elevated *FMR1* mRNA levels (15,26,49). As a further point regarding the influence of FMRP on the present observations, It has been recently reported that the variation of FMRP among individuals with normal *FMR1* alleles is >4-fold in the general population (38,64), in the absence of any clinical features of FXS.

GABA receptor signaling is critical to the regulation of neuronal firing activity. The application of GABA to cultured neurons reduced neuronal network activity (65), whereas the

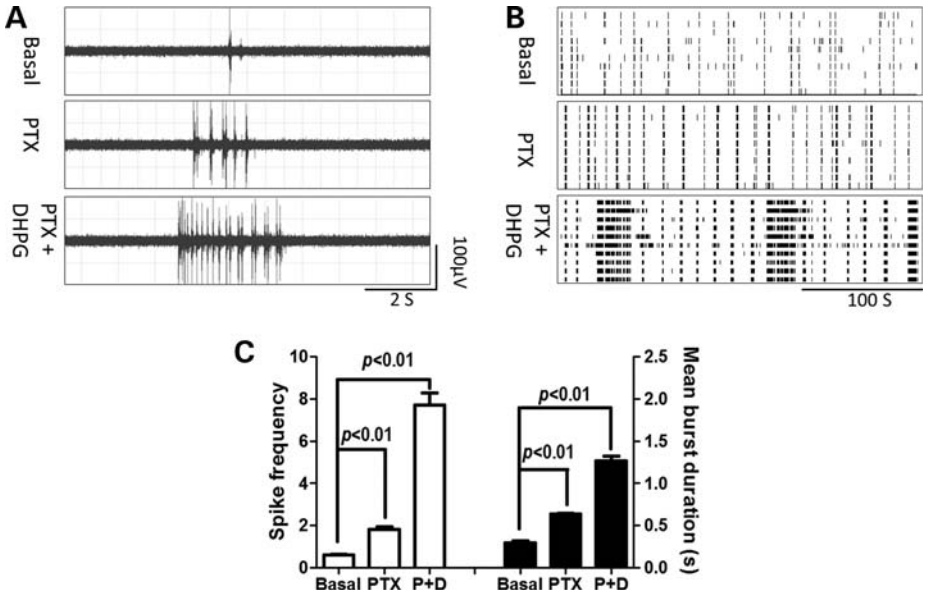

Figure 8. Picrotoxin, together with DHPG, induces CB firing pattern in WT hippocampal neurons. (**A**) Representative firing traces before and after WT hippocampal neurons were exposed to picrotoxin (100 μM) or a combination of picrotoxin (100 μM) and DHPG (10 μM), respectively. (**B**) Representative raster plots of the neuronal firing before and after picrotoxin or picrotoxin and DHPG exposure. (**C**) Quantification of the spike frequency (left *Y* axis) and mean burst duration (right *Y* axis) before and after exposure to picrotoxin or picrotoxin and DHPG exposure. These data were repeated twice in two independent cultures with similar results.

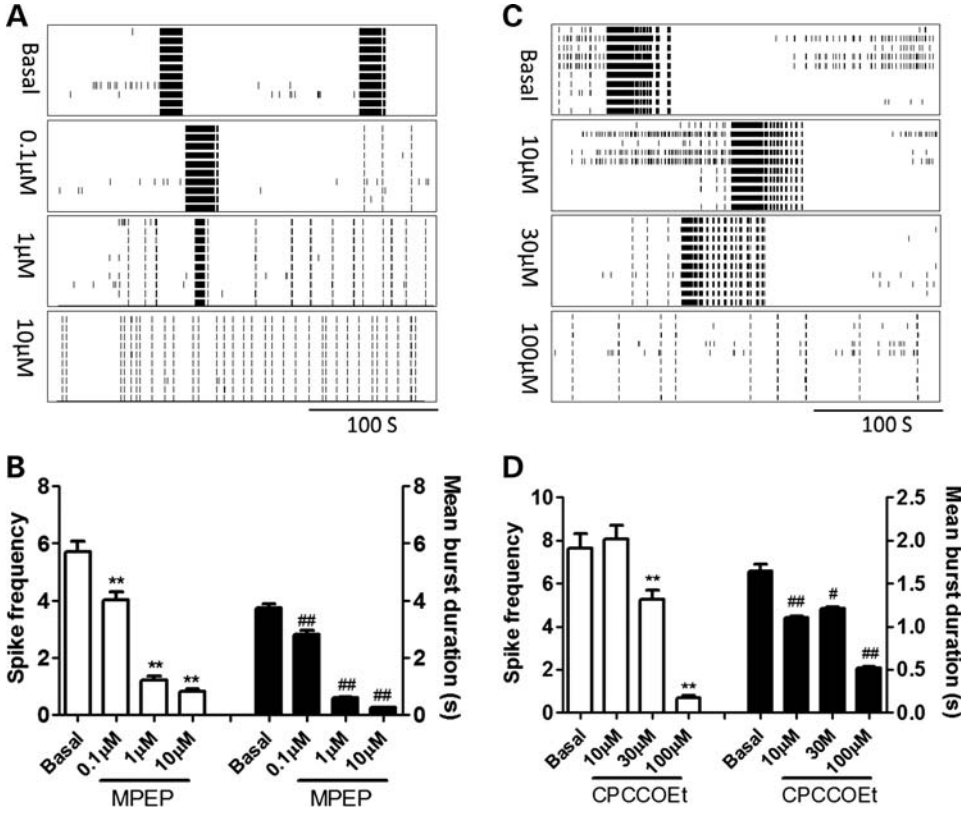

Figure 9. MPEP and CPCCOEt reversed the CB firing pattern in preCGG hippocampal neurons in a concentration-dependent manner. (**A** and **C**) Representative raster plots for the neuronal firing before and after preCGG hippocampal neurons were exposed to MPEP or CPCCOEt, respectively. (**B** and **D**) Quantification of the spike frequency (left *Y* axis) and mean burst duration (right *Y* axis) for preCGG hippocampal neurons before and during exposure to different concentrations of MPEP and CPCCOEt, respectively. These data were repeated twice in duplicate with similar results.

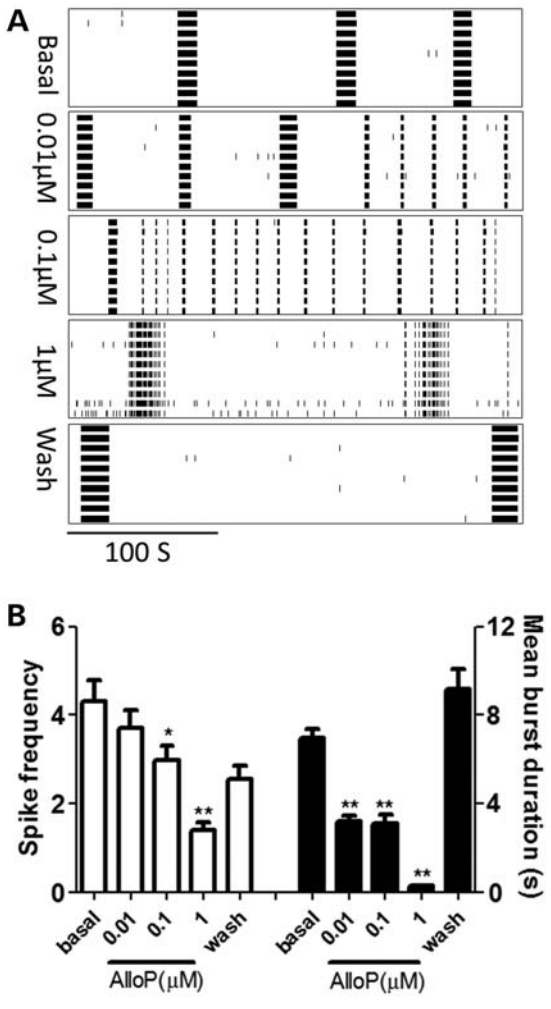

Figure 10. Allopregnanolone reversibly reduced the spike frequency and burst duration of the preCGG hippocampal neurons. (**A**) Representative raster plots for the neuronal firing of preCGG hippocampal neurons before and during exposure to as well as washout of allopregnanolone. (**B**) Quantification of the spike frequency (left *Y* axis) and mean burst duration (right *Y* axis) for preCGG hippocampal neurons before and during exposure to as well as after washout of allopregnanolone, respectively. Data were repeated two times with independent cultures.

inhibition of $GABA_A$ receptors by bicuculline, a competitive antagonist of $GABA_A$ receptors, elicited a highly synchronized, periodic burst firing pattern (65,66), similar to those we elicited in WT neurons exposed to picrotoxin. Altered mGluR5 receptor signaling has been demonstrated in the *Fmr1*KO FXS mouse model, where the mGluR5-dependent long-term synaptic depression is enhanced during the synaptic transmission (67). This enhancement was later proved to be due to excessive protein synthesis downstream of mGluR5 activation with the loss of FMRP expression, the latter normally acting as a negative regulator of mRNA translation (68). Here, we show that block of mGluR1/5 resolves CB firing behavior. However, mGluR1/5 signaling impairments that contribute to CB firing behavior in preCGG neurons occur in the presence of appreciable but reduced levels FMRP, and thus may be etiologically distinct from FXS, although may respond to medications now used for targeted treatment trials in FXS (69).

A finding of potential clinical importance for novel therapeutic prophylaxis of premutation-related disorders or FXTAS intervention is our observation that the neurosteroid allopregnanolone can mitigate CB firing patterns in a concentration-dependent and reversible manner. Collectively these data further support the concept that impaired mGluR1/5 and $GABA_A$ receptor signaling pathways contribute to physiologic impairments in preCGG neurons and identify novel intervention strategies for targeted treatment of premutation developmental disorders and FXTAS.

MATERIALS AND METHODS

Materials

Anti-VGAT and anti-VGLUT1 antibodies were purchased from Synaptic Systems GmbH (Goettingen, Germany). Mouse anti-β-actin antibody was from Cell Signaling Technology (Danvers, MA, USA). Chicken-anti-FMRP antibody was generated in P.J.H.'s laboratory (38). NewBlot Nitro Stripping Buffer, Odyssey Blocking Buffer and IRDye-labeled secondary antibody were from LI-COR Biotechnology (Lincoln, NE, USA). Fluo-4 and Pluronic F-127 were from Invitrogen (Carlsbad, CA, USA). L-*trans*-PDC, TBOA, MPEP, CPCCOEt, DHPG, NMDA and AMPA were from Tocris Bioscience (Ellisville, MO, USA). Allopregnanolone (3α-hydroxy-5α-pregnan-20-one) was synthesized by M.A.R. and characterized as >99% pure.

PreCGG mouse model

All preCGG KI and WT mice in the C57 B6 background were housed under standard vivarium conditions. PreCGG hemizygous male mice (150–190 CGG expansion repeat; average 170) were obtained by breeding homozygous preCGG females with preCGG hemizygous males from founders derived from Erasmus University (20). Male WT and preCGG pups delivered on the same day were used for paired cultures. The *FMR1* genotype was verified by PCR (36). All animal use protocols were approved by the University of California, Davis IACUC.

Genotyping

DNA was extracted from mouse tail, and genotyping of the *FMR1* expansion size was performed using the forward and reverse primers previously described (36).

Hippocampal neuron–astrocyte co-culture

Hippocampal astrocyte–neuron mixed cultures were obtained from postnatal day 0–1 (P0–1) WT or preCGG KI male pups. Mice were decapitated, their brains removed and hippocampi dissected in a sterile hood. Hippocampal neurons were dissociated and plated onto poly-L-lysine-coated 6-well plates or clear-bottom, black well, 96-well imaging plates (BD, Franklin Lakes, NJ, USA) at densities of 2×10^6/well or 1×10^5/well, respectively, as previously described (36). For microelectrode array (MEA) experiments, 60 μl of cell suspension at a density of 2×10^6 cells/ml was added as a drop to the

center of MEA to cover the 64 electrode probes. After 2 h incubation, a volume of 1.5 ml of serum-free neurobasal supplemented medium containing NS21 supplement, 0.5 mM L-glutamine and HEPES was added to each MEA. The medium was changed twice a week by replacing half volume of culture medium with serum-free neurobasal supplemented medium. The cells were maintained in an atmosphere at 37°C with 5% CO_2 and 95% humidity.

Hippocampal astrocytes culture

Enriched hippocampal astrocytes were obtained from P0–1 WT or preCGG KI male pups. The dissection and dissociation of the cells is the same as the neuronal preparation. After digestion and centrifugation as described for the isolation of neurons, cells were suspended in DMEM medium supplemented with 10% fetal bovine serum, 100 IU/ml penicillin and 0.10 mg/ml streptomycin, pH 7.4. Cells were plated onto poly-L-ornithine-coated T-75 culture flask at a density of $2–3 \times 10^6$ cells/flask and maintained in an incubator at 37°C with 5% CO_2 and 95% humidity. The culture medium was changed twice a week and the cells were used between 2 and 4 weeks and no more than three passages.

Western blot

The sample preparation for western blot was performed as described previously (70). Equal amounts (20 μg) of samples were loaded onto a 10% SDS–PAGE gel and transferred to a nitrocellulose membrane by electroblotting. The membranes were blocked with Odyssey Blocking Buffer (for VGLUT1 and VGAT antibodies) or 5% non-skimmed milk in PBS buffer + 0.1% Tween-20 (for the FMRP antibody) for 1.5–2 h at room temperature. After blocking, membranes were incubated overnight at 4°C in the primary antibody dilution (anti-VGAT, 1:5000; anti-VGLUT1, 1:10 000; anti-FMRP, 1:20 000 and anti-β-actin, 1:20 000). The blots were washed and incubated with the IRDye (800CW or 700CW)-labeled secondary antibody (1:10 000) for 1 h at room temperature. After washing with 0.1% Tween in PBS for five times, the membrane was scanned with the LI-COR Odyssey Infrared Imaging System (LI-COR Biotechnology). Densitometry was performed using the LI-COR Odyssey Infrared Imaging System application software 2.1. Membranes were stripped with NewBlot Nitro Stripping Buffer and reblotted for analysis of additional proteins.

Quantitative measurements of *Fmr1* mRNA levels

Total RNA from primary hippocampal cultures was isolated by a standard method (Trizol, Ambion, Inc., Austin, TX, USA). Precise estimates of *Fmr1* mRNA levels in total RNA were obtained by real-time PCR. Details of the method and its application to the study of *Fmr1* mRNAs are as described previously (22). The reference gene was β-glucoronidase (*GUS*). The analysis was repeated for three different RNA concentrations, in duplicate, and incorporated standards for each determination to compensate for any changes in reaction efficiency.

Ca^{2+} oscillation determination

The WT and premutation hippocampal neurons cultured in the same clear-bottom, 96-well imaging plate were used to determine the spontaneous Ca^{2+} oscillations as described previously (71).

MEA recording

All MEA recordings were performed at 37°C in culture medium without perfusion with the MED64 system (Alpha MED Scientific, Inc., Ibaraki, Osaka, Japan). The MED probe contains 64 electrodes in an 8 × 8 grid with an inter-electrode spacing of 150 μm. MEA probes were loaded in the MED-C03 chamber and the raw data were acquired using the Mobius software (Alpha MED Scientific, Inc., Ibaraki, Osaka, Japan). Signals from the amplifier were digitized at a rate of 20 kHz and using a high-pass filter (cutoff frequency of 100 Hz). Supplementary Material, Figure S1A shows single-spike waveforms from preCGG hippocampal neurons at 21 DIV. The Mobius software was used to detect spontaneous events that exceeded a threshold of −25 μV (Supplementary Material, Fig. S1B)—the typical peak-to-peak noise level of MEA electrodes was ±5–8 μV. The time stamps for each channel were then saved and exported to an Excel sheet. For raster plot as well as spike rate and burst analysis, data were imported into the NeuroExplorer software (version 4.0, NEX Technologies, Littleton, MA, USA) and analyzed using the raster or burst firing analysis function. For an activity to be defined as a burst, spikes had to occur within 350 ms of each other. In addition, a burst consisted of a minimum of four spikes with minimum burst duration of 100 ms. The minimum separation between bursts was set at 350 ms. Using this measurement, the burst duration is measured from the start of a burst until the gap to the next spike is more than 350 ms, so one repetitive burst may include multiple high-frequency bursts (Supplementary Material, Fig. S1C).

Data analysis

Graphing and statistical analysis were performed using the GraphPad Prism software (Version 5.0, GraphPad Software, Inc., San Diego, CA, USA). Statistical significance between different groups was calculated using Student's *t*-test or by an ANOVA and, where appropriate, a Dunnett's multiple comparison test. The *P*-values below 0.05% were considered significant. Kinetic parameters (K_m and V_{max}) for Glu uptake were determined by nonlinear regression analysis of the saturation curves, using the Michaelis–Menten equation.

SUPPLEMENTARY MATERIAL

Supplementary Material is available at *HMG* online.

ACKNOWLEDGEMENTS

The authors wish to express their gratitude to the families who have supported our research in developmental disorders. Drs Rob Willemsen (Department of Clinical Genetics,

Erasmus MC, Rotterdam, The Netherlands) and Rob Berman (Department of Neurological Surgery, UC Davis) are gratefully acknowledged for providing the preCGG mice.

Conflicts of Interest statement. R.J.H. has received funding from Novartis, Roche, Seaside Therapeutics and Forest to carry out targeted treatment trial in those with FXS or autism. She is also on the FXS Treatment Advisory Board of Novartis. The other authors have no conflicts of interest to declare.

FUNDING

This project was supported by National Institutes of Health (grant numbers RC1 AG036022 to P.J.H. and I.N.P., UL1 DE019583 to P.J.H., RL1 AG032119 to P.J.H. and I.N.P., RL1 AG032115 to R.J.H., R01 ES011269 to I.N.P., R21 NS072094 to M.A.R.), Congressionally Directed Medical Research Programs (grant number W81XWH-09-1-0746 to M.A.R.) and an unrestricted research grant from the J.B. Johnson Foundation to I.N.P.

REFERENCES

1. Jacquemont, S., Hagerman, R.J., Hagerman, P.J. and Leehey, M.A. (2007) Fragile-X syndrome and fragile X-associated tremor/ataxia syndrome: two faces of FMR1. *Lancet Neurol.*, **6**, 45–55.
2. Hagerman, R., Au, J. and Hagerman, P. (2011) FMR1 premutation and full mutation molecular mechanisms related to autism. *J. Neurodev. Disord.*, **3**, 211–224.
3. Oostra, B.A. and Willemsen, R. (2009) FMR1: a gene with three faces. *Biochim. Biophys. Acta*, **1790**, 467–477.
4. Brouwer, J.R., Severijnen, E., de Jong, F.H., Hessl, D., Hagerman, R.J., Oostra, B.A. and Willemsen, R. (2008) Altered hypothalamus-pituitary-adrenal gland axis regulation in the expanded CGG-repeat mouse model for fragile X-associated tremor/ataxia syndrome. *Psychoneuroendocrinology*, **33**, 863–873.
5. Fu, Y.H., Kuhl, D.P., Pizzuti, A., Pieretti, M., Sutcliffe, J.S., Richards, S., Verkerk, A.J., Holden, J.J., Fenwick, R.G. Jr, Warren, S.T. *et al.* (1991) Variation of the CGG repeat at the fragile X site results in genetic instability: resolution of the Sherman paradox. *Cell*, **67**, 1047–1058.
6. Goodlin-Jones, B.L., Tassone, F., Gane, L.W. and Hagerman, R.J. (2004) Autistic spectrum disorder and the fragile X premutation. *J. Dev. Behav. Pediatr.*, **25**, 392–398.
7. Hessl, D., Tassone, F., Loesch, D.Z., Berry-Kravis, E., Leehey, M.A., Gane, L.W., Barbato, I., Rice, C., Gould, E., Hall, D.A. *et al.* (2005) Abnormal elevation of FMR1 mRNA is associated with psychological symptoms in individuals with the fragile X premutation. *Am. J. Med. Genet. B Neuropsychiatr. Genet.*, **139B**, 115–121.
8. Farzin, F., Perry, H., Hessl, D., Loesch, D., Cohen, J., Bacalman, S., Gane, L., Tassone, F., Hagerman, P. and Hagerman, R. (2006) Autism spectrum disorders and attention-deficit/hyperactivity disorder in boys with the fragile X premutation. *J. Dev. Behav. Pediatr.*, **27**, S137–S144.
9. Hagerman, R.J. (2006) Lessons from fragile X regarding neurobiology, autism, and neurodegeneration. *J. Dev. Behav. Pediatr.*, **27**, 63–74.
10. Wittenberger, M.D., Hagerman, R.J., Sherman, S.L., McConkie-Rosell, A., Welt, C.K., Rebar, R.W., Corrigan, E.C., Simpson, J.L. and Nelson, L.M. (2007) The FMR1 premutation and reproduction. *Fertil. Steril.*, **87**, 456–465.
11. Amiri, K., Hagerman, R.J. and Hagerman, P.J. (2008) Fragile X-associated tremor/ataxia syndrome: an aging face of the fragile X gene. *Arch. Neurol.*, **65**, 19–25.
12. Brouwer, J.R., Willemsen, R. and Oostra, B.A. (2009) The FMR1 gene and fragile X-associated tremor/ataxia syndrome. *Am. J. Med. Genet. B Neuropsychiatr. Genet.*, **150B**, 782–798.
13. Tassone, F., Adams, J., Berry-Kravis, E.M., Cohen, S.S., Brusco, A., Leehey, M.A., Li, L., Hagerman, R.J. and Hagerman, P.J. (2007) CGG repeat length correlates with age of onset of motor signs of the fragile X-associated tremor/ataxia syndrome (FXTAS). *Am. J. Med. Genet. B Neuropsychiatr. Genet.*, **144B**, 566–569.
14. Song, F.J., Barton, P., Sleightholme, V., Yao, G.L. and Fry-Smith, A. (2003) Screening for fragile X syndrome: a literature review and modelling study. *Health. Technol. Assess.*, **7**, 1–106.
15. Hagerman, P.J. (2008) The fragile X prevalence paradox. *J. Med. Genet.*, **45**, 498–499.
16. Rodriguez-Revenga, L., Madrigal, I., Pagonabarraga, J., Xuncla, M., Badenas, C., Kulisevsky, J., Gomez, B. and Mila, M. (2009) Penetrance of FMR1 premutation associated pathologies in fragile X syndrome families. *Eur. J. Hum. Genet.*, **17**, 1359–1362.
17. Jacquemont, S., Farzin, F., Hall, D., Leehey, M., Tassone, F., Gane, L., Zhang, L., Grigsby, J., Jardini, T., Lewin, F. *et al.* (2004) Aging in individuals with the FMR1 mutation. *Am. J. Ment. Retard.*, **109**, 154–164.
18. Berry-Kravis, E., Abrams, L., Coffey, S.M., Hall, D.A., Greco, C., Gane, L.W., Grigsby, J., Bourgeois, J.A., Finucane, B., Jacquemont, S. *et al.* (2007) Fragile X-associated tremor/ataxia syndrome: clinical features, genetics, and testing guidelines. *Mov. Disord.*, **22**, 2018–2030, quiz 2140.
19. Bourgeois, J.A., Coffey, S.M., Rivera, S.M., Hessl, D., Gane, L.W., Tassone, F., Greco, C., Finucane, B., Nelson, L., Berry-Kravis, E. *et al.* (2009) A review of fragile X premutation disorders: expanding the psychiatric perspective. *J. Clin. Psychiatry*, **70**, 852–862.
20. Willemsen, R., Hoogeveen-Westerveld, M., Reis, S., Holstege, J., Severijnen, L.A., Nieuwenhuizen, I.M., Schrier, M., van Unen, L., Tassone, F., Hoogeveen, A.T. *et al.* (2003) The FMR1 CGG repeat mouse displays ubiquitin-positive intranuclear neuronal inclusions; implications for the cerebellar tremor/ataxia syndrome. *Hum. Mol. Genet.*, **12**, 949–959.
21. Brouwer, J.R., Mientjes, E.J., Bakker, C.E., Nieuwenhuizen, I.M., Severijnen, L.A., Van der Linde, H.C., Nelson, D.L., Oostra, B.A. and Willemsen, R. (2007) Elevated Fmr1 mRNA levels and reduced protein expression in a mouse model with an unmethylated Fragile X full mutation. *Exp. Cell Res.*, **313**, 244–253.
22. Tassone, F., Hagerman, R.J., Taylor, A.K., Gane, L.W., Godfrey, T.E. and Hagerman, P.J. (2000) Elevated levels of FMR1 mRNA in carrier males: a new mechanism of involvement in the fragile-X syndrome. *Am. J. Hum. Genet.*, **66**, 6–15.
23. Greco, C.M., Hagerman, R.J., Tassone, F., Chudley, A.E., Del Bigio, M.R., Jacquemont, S., Leehey, M. and Hagerman, P.J. (2002) Neuronal intranuclear inclusions in a new cerebellar tremor/ataxia syndrome among fragile X carriers. *Brain*, **125**, 1760–1771.
24. Greco, C.M., Berman, R.F., Martin, R.M., Tassone, F., Schwartz, P.H., Chang, A., Trapp, B.D., Iwahashi, C., Brunberg, J., Grigsby, J. *et al.* (2006) Neuropathology of fragile X-associated tremor/ataxia syndrome (FXTAS). *Brain*, **129**, 243–255.
25. Tassone, F., Iwahashi, C. and Hagerman, P.J. (2004) FMR1 RNA within the intranuclear inclusions of fragile X-associated tremor/ataxia syndrome (FXTAS). *RNA Biol.*, **1**, 103–105.
26. Arocena, D.G., Iwahashi, C.K., Won, N., Beilina, A., Ludwig, A.L., Tassone, F., Schwartz, P.H. and Hagerman, P.J. (2005) Induction of inclusion formation and disruption of lamin A/C structure by premutation CGG-repeat RNA in human cultured neural cells. *Hum. Mol. Genet.*, **14**, 3661–3671.
27. Hashem, V., Galloway, J.N., Mori, M., Willemsen, R., Oostra, B.A., Paylor, R. and Nelson, D.L. (2009) Ectopic expression of CGG containing mRNA is neurotoxic in mammals. *Hum. Mol. Genet.*, **18**, 2443–2451.
28. Berman, R.F. and Willemsen, R. (2009) Mouse models of fragile x-associated tremor ataxia. *J. Investig. Med.*, **57**, 837–841.
29. Entezam, A., Biacsi, R., Orrison, B., Saha, T., Hoffman, G.E., Grabczyk, E., Nussbaum, R.L. and Usdin, K. (2007) Regional FMRP deficits and large repeat expansions into the full mutation range in a new Fragile X premutation mouse model. *Gene*, **395**, 125–134.
30. Hunsaker, M.R., Goodrich-Hunsaker, N.J., Willemsen, R. and Berman, R.F. (2010) Temporal ordering deficits in female CGG KI mice heterozygous for the fragile X premutation. *Behav. Brain Res.*, **213**, 263–268.
31. Hunsaker, M.R., von Leden, R.E., Ta, B.T., Goodrich-Hunsaker, N.J., Arque, G., Kim, K., Willemsen, R. and Berman, R.F. (2011) Motor deficits on a ladder rung task in male and female adolescent and adult CGG knock-in mice. *Behav. Brain Res.*, **222**, 117–121.
32. Qin, M., Entezam, A., Usdin, K., Huang, T., Liu, Z.H., Hoffman, G.E. and Smith, C.B. (2011) A mouse model of the fragile X premutation: effects

on behavior, dendrite morphology, and regional rates of cerebral protein synthesis. *Neurobiol. Dis.*, **42**, 85–98.
33. Hunsaker, M.R., Greco, C.M., Tassone, F., Berman, R.F., Willemsen, R., Hagerman, R.J. and Hagerman, P.J. (2011) Rare intranuclear inclusions in the brains of 3 older adult males with fragile x syndrome: implications for the spectrum of fragile x-associated disorders. *J. Neuropathol. Exp. Neurol.*, **70**, 462–469.
34. Wenzel, H.J., Hunsaker, M.R., Greco, C.M., Willemsen, R. and Berman, R.F. (2010) Ubiquitin-positive intranuclear inclusions in neuronal and glial cells in a mouse model of the fragile X premutation. *Brain Res.*, **1318**, 155–166.
35. Cunningham, C.L., Martinez Cerdeno, V., Navarro Porras, E., Prakash, A.N., Angelastro, J.M., Willemsen, R., Hagerman, P.J., Pessah, I.N., Berman, R.F. and Noctor, S.C. (2011) Premutation CGG-repeat expansion of the Fmr1 gene impairs mouse neocortical development. *Hum. Mol. Genet.*, **20**, 64–79.
36. Chen, Y., Tassone, F., Berman, R.F., Hagerman, P.J., Hagerman, R.J., Willemsen, R. and Pessah, I.N. (2010) Murine hippocampal neurons expressing Fmr1 gene premutations show early developmental deficits and late degeneration. *Hum. Mol. Genet.*, **19**, 196–208.
37. D'Hulst, C., Heulens, I., Brouwer, J.R., Willemsen, R., De Geest, N., Reeve, S.P., De Deyn, P.P., Hassan, B.A. and Kooy, R.F. (2009) Expression of the GABAergic system in animal models for fragile X syndrome and fragile X associated tremor/ataxia syndrome (FXTAS). *Brain Res.*, **1253**, 176–183.
38. Iwahashi, C., Tassone, F., Hagerman, R.J., Yasui, D., Parrott, G., Nguyen, D., Mayeur, G. and Hagerman, P.J. (2009) A quantitative ELISA assay for the fragile x mental retardation 1 protein. *J. Mol. Diagn.*, **11**, 281–289.
39. Johnstone, A.F., Gross, G.W., Weiss, D.G., Schroeder, O.H., Gramowski, A. and Shafer, T.J. (2010) Microelectrode arrays: a physiologically based neurotoxicity testing platform for the 21st century. *Neurotoxicology*, **31**, 331–350.
40. Tanaka, T., Saito, H. and Matsuki, N. (1996) Intracellular calcium oscillation in cultured rat hippocampal neurons: a model for glutamatergic neurotransmission. *Jpn J. Pharmacol.*, **70**, 89–93.
41. Chaudhry, F.A., Reimer, R.J., Bellocchio, E.E., Danbolt, N.C., Osen, K.K., Edwards, R.H. and Storm-Mathisen, J. (1998) The vesicular GABA transporter, VGAT, localizes to synaptic vesicles in sets of glycinergic as well as GABAergic neurons. *J. Neurosci.*, **18**, 9733–9750.
42. Balschun, D., Moechars, D., Callaerts-Vegh, Z., Vermaercke, B., Van Acker, N., Andries, L. and D'Hooge, R. (2010) Vesicular glutamate transporter VGLUT1 has a role in hippocampal long-term potentiation and spatial reversal learning. *Cereb. Cortex*, **20**, 684–693.
43. McIntire, S.L., Reimer, R.J., Schuske, K., Edwards, R.H. and Jorgensen, E.M. (1997) Identification and characterization of the vesicular GABA transporter. *Nature*, **389**, 870–876.
44. Bellocchio, E.E., Reimer, R.J., Fremeau, R.T. Jr and Edwards, R.H. (2000) Uptake of glutamate into synaptic vesicles by an inorganic phosphate transporter. *Science*, **289**, 957–960.
45. Kudela, P., Franaszczuk, P.J. and Bergey, G.K. (2003) Changing excitation and inhibition in simulated neural networks: effects on induced bursting behavior. *Biol. Cybern.*, **88**, 276–285.
46. Rothstein, J.D., Dykes-Hoberg, M., Pardo, C.A., Bristol, L.A., Jin, L., Kuncl, R.W., Kanai, Y., Hediger, M.A., Wang, Y., Schielke, J.P. *et al.* (1996) Knockout of glutamate transporters reveals a major role for astroglial transport in excitotoxicity and clearance of glutamate. *Neuron*, **16**, 675–686.
47. Frega, M., Pasquale, V., Tedesco, M., Marcoli, M., Contestabile, A., Nanni, M., Bonzano, L., Maura, G. and Chiappalone, M. (2012) Cortical cultures coupled to micro-electrode arrays: a novel approach to perform *in vitro* excitotoxicity testing. *Neurotoxicol. Teratol.*, **34**, 116–127.
48. Kokate, T.G., Svensson, B.E. and Rogawski, M.A. (1994) Anticonvulsant activity of neurosteroids: correlation with gamma-aminobutyric acid-evoked chloride current potentiation. *J. Pharmacol. Exp. Ther.*, **270**, 1223–1229.
49. Brouwer, J.R., Huizer, K., Severijnen, L.A., Hukema, R.K., Berman, R.F., Oostra, B.A. and Willemsen, R. (2008) CGG-repeat length and neuropathological and molecular correlates in a mouse model for fragile X-associated tremor/ataxia syndrome. *J. Neurochem.*, **107**, 1671–1682.
50. Hessl, D., Wang, J.M., Schneider, A., Koldewyn, K., Le, L., Iwahashi, C., Cheung, K., Tassone, F., Hagerman, P.J. and Rivera, S.M. (2011) Decreased fragile X mental retardation protein expression underlies amygdala dysfunction in carriers of the fragile X premutation. *Biol. Psychiatry*, **70**, 859–865.
51. Chonchaiya, W., Au, J., Schneider, A., Hessl, D., Harris, S.W., Laird, M., Mu, Y., Tassone, F., Nguyen, D.V. and Hagerman, R.J. (2012) Increased prevalence of seizures in boys who were probands with the FMR1 premutation and co-morbid autism spectrum disorder. *Hum. Genet.*, **131**, 581–589.
52. Komuro, H. and Kumada, T. (2005) Ca^{2+} transients control CNS neuronal migration. *Cell Calcium*, **37**, 387–393.
53. Berridge, M.J. (2006) Calcium microdomains: organization and function. *Cell Calcium*, **40**, 405–412.
54. Higley, M.J. and Sabatini, B.L. (2008) Calcium signaling in dendrites and spines: practical and functional considerations. *Neuron*, **59**, 902–913.
55. Lohmann, C., Finski, A. and Bonhoeffer, T. (2005) Local calcium transients regulate the spontaneous motility of dendritic filopodia. *Nat. Neurosci.*, **8**, 305–312.
56. Segal, I., Korkotian, I. and Murphy, D.D. (2000) Dendritic spine formation and pruning: common cellular mechanisms? *Trends Neurosci.*, **23**, 53–57.
57. Herzog, E., Bellenchi, G.C., Gras, C., Bernard, V., Ravassard, P., Bedet, C., Gasnier, B., Giros, B. and El Mestikawy, S. (2001) The existence of a second vesicular glutamate transporter specifies subpopulations of glutamatergic neurons. *J. Neurosci.*, **21**, RC181.
58. Kaneko, T. and Fujiyama, F. (2002) Complementary distribution of vesicular glutamate transporters in the central nervous system. *Neurosci. Res.*, **42**, 243–250.
59. Fremeau, R.T. Jr, Kam, K., Qureshi, T., Johnson, J., Copenhagen, D.R., Storm-Mathisen, J., Chaudhry, F.A., Nicoll, R.A. and Edwards, R.H. (2004) Vesicular glutamate transporters 1 and 2 target to functionally distinct synaptic release sites. *Science*, **304**, 1815–1819.
60. Minelli, A., Edwards, R.H., Manzoni, T. and Conti, F. (2003) Postnatal development of the glutamate vesicular transporter VGLUT1 in rat cerebral cortex. *Brain Res. Dev. Brain Res.*, **140**, 309–314.
61. Fung, S.J., Webster, M.J. and Weickert, C.S. (2011) Expression of VGluT1 and VGAT mRNAs in human dorsolateral prefrontal cortex during development and in schizophrenia. *Brain Res.*, **1388**, 22–31.
62. Tessier, C.R. and Broadie, K. (2011) The fragile X mental retardation protein developmentally regulates the strength and fidelity of calcium signaling in *Drosophila* mushroom body neurons. *Neurobiol. Dis.*, **41**, 147–159.
63. Deng, P.Y., Sojka, D. and Klyachko, V.A. (2011) Abnormal presynaptic short-term plasticity and information processing in a mouse model of fragile X syndrome. *J. Neurosci.*, **31**, 10971–10982.
64. Lessard, M., Chouiali, A., Drouin, R., Sebire, G. and Corbin, F. (2012) Quantitative measurement of FMRP in blood platelets as a new screening test for fragile X syndrome. *Clin. Genet.*, In press.
65. Gross, G.W., Rhoades, B.K., Azzazy, H.M. and Wu, M.C. (1995) The use of neuronal networks on multielectrode arrays as biosensors. *Biosens. Bioelectron.*, **10**, 553–567.
66. Keefer, E.W., Gramowski, A. and Gross, G.W. (2001) NMDA receptor-dependent periodic oscillations in cultured spinal cord networks. *J. Neurophysiol.*, **86**, 3030–3042.
67. Huber, K.M., Gallagher, S.M., Warren, S.T. and Bear, M.F. (2002) Altered synaptic plasticity in a mouse model of fragile X mental retardation. *Proc. Natl Acad. Sci. USA*, **99**, 7746–7750.
68. Bear, M.F., Huber, K.M. and Warren, S.T. (2004) The mGluR theory of fragile X mental retardation. *Trends Neurosci.*, **27**, 370–377.
69. Wang, L.W., Berry-Kravis, E. and Hagerman, R.J. (2010) Fragile X: leading the way for targeted treatments in autism. *Neurotherapeutics*, **7**, 264–274.
70. Cao, Z., George, J., Baden, D.G. and Murray, T.F. (2007) Brevetoxin-induced phosphorylation of Pyk2 and Src in murine neocortical neurons involves distinct signaling pathways. *Brain Res.*, **1184**, 17–27.
71. Cao, Z., LePage, K.T., Frederick, M.O., Nicolaou, K.C. and Murray, T.F. (2010) Involvement of caspase activation in azaspiracid-induced neurotoxicity in neocortical neurons. *Toxicol. Sci.*, **114**, 323–334.